

Experimental Investigation of a Sensible Thermal Energy Storage System



Vishwa Deepak Kumar, Yudhisther Surolia, Sudipto Mukhopadhyay,
and Laltu Chandra

1 Introduction

Solar energy is a promising renewable source to meet the growing energy demand. Using concentrated solar thermal (CST) technologies, solar energy can be harnessed to meet thermal as well as electrical demand Häberle (2012); Blanco and Miller (2017). CST technologies need to concentrate sunlight. Optical concentration is achieved using the direct beam irradiance component. Direct beam irradiance is generally quantified by the amount of solar radiation received per unit area by a surface normal to the sun and is called direct normal irradiance (DNI). The DNI distribution across the globe varies with the highest values around the subtropics. For example, DNI map of India NREL (2021) shows the abundance of solar radiation in Rajasthan and Gujarat, with an availability of more than $5.5 \text{ kWh/m}^2/\text{day}$. In CST technologies, the DNI is concentrated onto a receiver using curved reflectors, like parabolic trough, linear Fresnel, heliostat, and dish, etc. In heliostat-based CST system, DNI is concentrated onto a receiver, viz. open or closed volumetric air receiver. The open volumetric air receiver (OVAR)-based solar towers use ambient air as heat transfer fluid (HTF) and are capable to heat air beyond a temperature of 800°C Pitz-Paal et al. (1997); Hoffschmidt et al. (2003); Ávila Marín (2011); Sharma et al. (2014). Thus, OVAR-based central tower technology can be used for metals processing operations, such as heat treatment and soaking. Sharma et al. Sharma et al. (2015) proposed the novel concept of a solar convective furnace (SCF) which is capable of heat treatment of metal via forced convection. In this system, hot air from OVAR is transported to a SCF through thermal energy storage (TES).

V. D. Kumar · Y. Surolia · S. Mukhopadhyay
Department of Mechanical Engineering, Indian Institute of Technology Jodhpur,
Jodhpur, Rajasthan 342037, India

L. Chandra (✉)
Department of Mechanical Engineering, IIT BHU Varanasi, Varanasi 221 005, India
e-mail: chandra.mec@iitbhu.ac.in

© The Author(s), under exclusive license to Springer Nature Singapore Pte Ltd. 2021
H. Tyagi et al. (eds.), *New Research Directions in Solar Energy Technologies*,
Energy, Environment, and Sustainability,
https://doi.org/10.1007/978-981-16-0594-9_13

A solar air tower simulator (SATS) facility is installed at IIT Jodhpur for assessment of this integrated concept. It consists of all the necessary sub-systems, such as OVAR, two TES viz. primary and secondary, cross-flow heat exchanger, and SCF. This facility is used for the experimental investigation of sub-systems. The mounted SCF is a part scaled-down model of retrofitted solar convective furnace Patidar et al. (2015, 2017). In the SATS facility, hot air is generated in OVAR through Joule heating and transported to TES or SCF through insulated pipes.

Due to intermittent nature of solar energy, TES is essential for a plant to run continuously without interruptions Fath (1998); Powell and Edgar (2012). Depending upon the duration of the heat storage, TES can have capacity to cater from diurnal to annual requirements. Some of the criteria for selecting a storage material are as follows:

- High thermal conductivity and high thermal diffusivity.
- Abundant and cheap.
- Non-explosive and non-corrosive in nature.
- Environment friendly.
- Stable under various loading conditions.

Two most commonly used thermal energy storage methods are discussed below briefly.

Latent heat thermal energy storage (LHTES) also called phase change storage as they have the capability to absorb or release energy with change in physical state. The energy storage density is inversely proportional to volume. A large amount of heat is generally stored during the phase change process nearly at a constant temperature and this directly related to latent heat of a storage medium. The main advantage of using this over sensible storage system is that it has a high energy storage density. Initially, it behaves as sensible heat storage system when temperature rises linearly, and then, it stores heat at constant temperature with phase change Sarbu and Sebarchievici (2018). Some commonly used phase change materials (PCM) are salt hydrates, fluorides, nitrides, chlorides, paraffins, and fatty acids Pielichowska and Pielichowski (2014). The LHTES system can be mathematically described as below:

$$Q_s = \int_{T_i}^{T_m} mc_{ps} dt + mf \Delta q + \int_{T_m}^{T_f} mc_{pl} dT \quad (1)$$

$$Q_s = mc_{ps}(T_m - T_i) + mf \Delta q + mc_{pl}(T_f - T_m) \quad (2)$$

where

m = mass of the phase change medium (kg)

T_i = initial temperature of the storage medium ($^{\circ}\text{C}$)

T_f = freezing temperature of the storage medium ($^{\circ}\text{C}$)

T_m = melting emperature of the storage medium ($^{\circ}\text{C}$)

f = melt fraction

δq = latent heat of fusion (J/kg)

Table 1 Characteristics of some common sensible heat storage solid materials Tian and Zhao (2013)

Storage Material	Working Temperature (°C)	Density (kg/m ³)	Specific heat (kJ/kg °C)	Thermal Conductivity (W/m K)
Sand-rock minerals	200–300	1700	1.30	1.0
Reinforced concrete	200–400	2200	0.85	1.5
Cast iron	200–400	7200	0.56	37.0
NaCl	200–500	2160	0.85	7.0
Cast steel	200–700	7800	0.60	40.0
Silica fire bricks	200–700	1820	1.00	1.5
Magnesia fire bricks	200–1200	3000	1.15	5.0

C_{ps} = average specific heat of solid phase between T_i and T_m (J/kg K)

C_{pl} = average specific heat of liquid phase between T_m and T_f (J/kg K)

Sensible heat thermal energy storage (SHTES) is one of the simplest methods in which energy is stored by heating or cooling a storage medium which may be solid or liquid. TES systems for sensible heat are commonly inexpensive as they consist of a simple enclosure for the storage medium and the equipment to charge/discharge. Storage media (e.g., water, soil, rocks, concrete, or molten salts) are generally commonly available and relatively cheap. Table 1 shows some of the most widely used solid SHTES materials and their properties. However, the container of the storage material requires effective thermal insulation, which may increase the TES cost Sarbu and Sebarchievici (2018).

For large-scale applications, underground storage of sensible heat in solid and liquid media is used. The two main advantages of SHTES are that firstly, it is cheap and secondly, it is environment friendly. It utilizes the heat capacity of storage medium and temperature of the medium changes during charging and discharging. The working principle of SHTES system can be mathematically described as below:

$$Q_s = \int_{T_i}^{T_f} mc_p dT = mc_p(T_f - T_i) \tag{3}$$

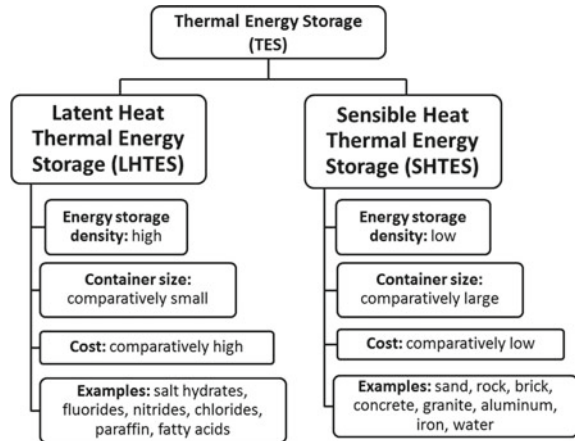
In above equation, the amount of heat stored by storage medium depends upon the quantity of the storage medium, specific heat of the medium, and the temperature change of the medium.

Q_s = amount of heat stored in Joule (J)

m = mass of the storage medium (kg)

C_p = specific heat of the storage medium (J/kg K)

Fig. 1 Comparison of LHTES and SHTES systems



T_i = initial temperature of the storage medium ($^{\circ}\text{C}$)

T_f = final temperature of the storage medium ($^{\circ}\text{C}$)

The main differences between LHTES and SHTES system are depicted in Fig. 1.

SHTES is widely deployed in practical applications and thus of present interest. In the SATS system studied here, both the TES are of SHTES type. The energy storage material used in this system is pebbles. The primary TES stores the heat generated in OVAR and supplies to SCF. The secondary storage recovers waste heat of air leaving from the furnace. The TES is very crucial in the overall operation of the SCF. The energy storage capacity of the TES and their charging/discharging capacity have to be measured over the time. In this work, secondary TES which is used for recovering waste heat is experimentally investigated. First, the experimental setup along with the construction of the secondary TES is described. Next, the experimental methodology for investigating the charging and discharging of the secondary TES is presented. This is followed by presentation of the experimental results obtained during the charging and discharging of the secondary TES. Lastly, the energy balance of the secondary TES, and then, main conclusions are summarized.

2 Experimental Setup

Solar air tower simulator (SATS) experiment setup of 4 kW is installed at IIT Jodhpur. Experimental setup is shown below in Fig. 2. The main components of the setup are:

- Open volumetric air receiver (OVAR).
- Primary TES system.
- Solar convective furnace.
- Secondary TES system.

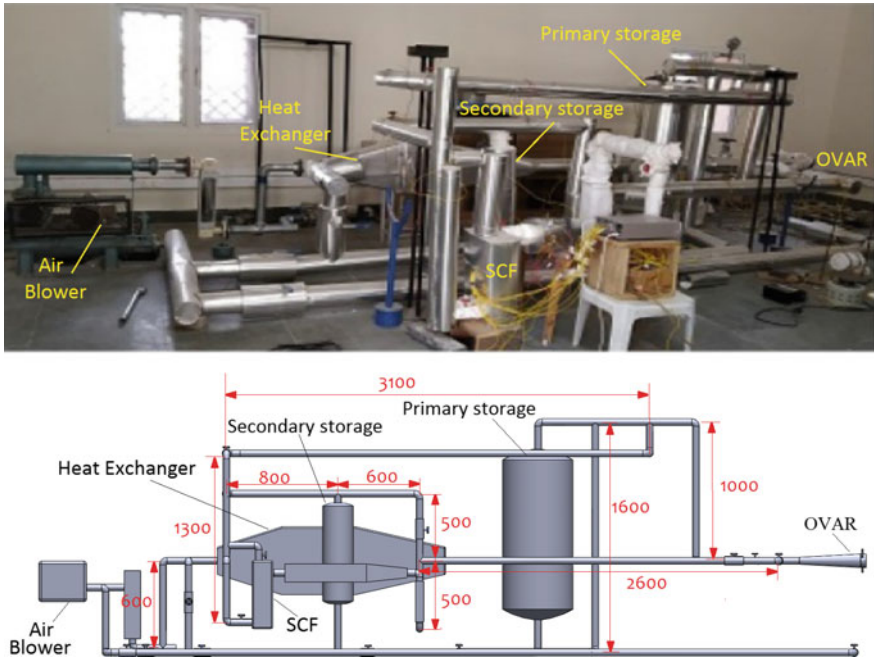


Fig. 2 Solar air tower simulator (SATS) setup at IIT Jodhpur (top) and its schematic with dimensions in mm (bottom)

- Air blower.
- Heat exchanger.

OVAR is the main component of the SATS where concentrated solar irradiation is incident and the thermal energy is absorbed for operation of the system. The OVAR is comprised of straight-pore-based absorbers and provides air at a high temperature. In order to perform experiments under controlled energy input, instead of concentrated irradiation, the receiver is heated by Joule heating. Nichrome wire is wrapped on the absorber circumference, for the Joule heating and wrapped with Kapton tape for electrical insulation to avoid short circuiting. The heat transfer fluid (HTF), which is air in this case, is sucked by the help of variable frequency drive twin lobe blower. It is installed to draw in air from the receiver to the entire system. Variable frequency drive controls the speed of motor to set a particular mass of air to be drawn in the system. To measure mass flow rate, rotameter is mounted before the air gets heated in order to prevent heat damage.

A cross-flow heat exchanger is also incorporated in the SATS to exchange heat with other fluids which can be used for other heating applications. With help of pipe valve arrangement, direction of HTF flow can be changed. HTF flow from OVAR to primary storage where heat can be stored and further utilized or it pass to the solar convective furnace. Solar convective furnace (SCF) is used for metal processing

like tempering, annealing, soaking. From solar convective furnace, HTF flows to the atmosphere through secondary thermal energy storage (TES) system. Schematic of SATS setup with the various dimensions are also shown in Fig. 2.

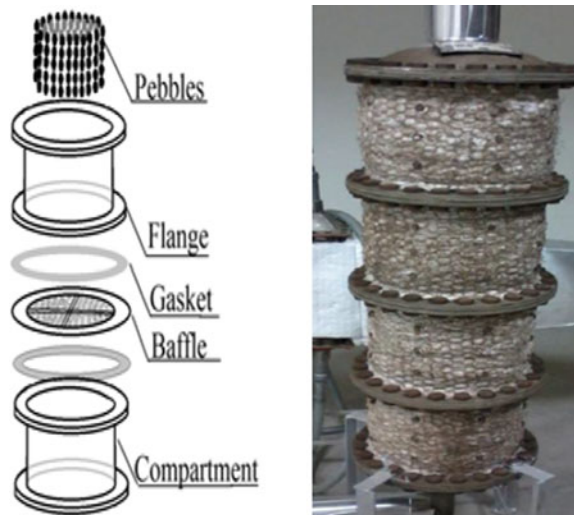
2.1 Thermal Energy Storage

As shown in Fig. 2, there are two heat storage systems: primary and secondary thermal energy storage. Both the TES are of SHTES type. The storage is built using pebbles enclosed in metal structure with insulation cover. The hot air can be directly introduced to the furnace or through pebble-bed primary thermal energy storage. The primary, high capacity, thermal energy storage is charged by introducing the generated hot air from receiver. The function of the primary TES is to supply hot air to SCF through its discharging. Thus, the primary storage is use to store heat for the metal processing operation with a sustained heating.

The secondary storage is typically used for waste heat recovery. The size of secondary storage is half of the primary storage, and heat storage capacity of secondary storage is 1/8 of the primary storage. The enthalpy of the fluid at outlet of the SCF is less than that at the outlet of the heater. This is because as the HTF passes through the SCF, it loses enthalpy during the metal processing as well heat is transferred to the system. However, the HTF still has sufficient energy which will be lost to ambient on exit from the SATS. This can be significant depending on the enthalpy of the HTF at outlet of solar convective furnace. The secondary TES serves to extract this enthalpy before it exits into the atmosphere, and this in turn improves the efficiency of the system.

The exploded view of the secondary TES is shown in Fig. 3. It consists of four cast iron cylindrical compartments for easy handling and packing of material connected

Fig. 3 TES: Exploded view (left) and assembly before enclosing (right)



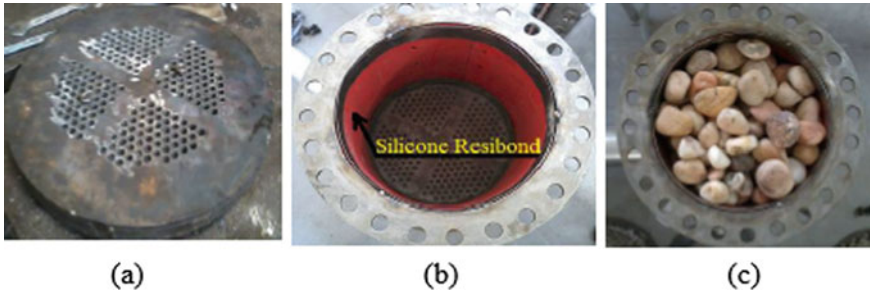


Fig. 4 Components of TES: **a** Baffle **b** empty compartment with resin bond **c** compartment filled with pebbles

Table 2 Secondary thermal energy storage design parameters

Parameter	Value
Length of compartment (mm)	125
Diameter of compartment (mm)	125
Number of compartment	4
Gap between two compartment (mm)	11
No of holes in baffle	192
Diameter of pebble (mm)	20
Inlet and outlet pipe diameter (mm)	50

with each other with the help of flange. For uniform distribution of HTF in every compartment, a baffle (porous plate) of thickness 10mm is used. Gasket is also used to ensure no leakage of air. To ensure perfect insulation, storage system is surrounded by silicone resin bond sheet from inside and glass wool on the outside. The baffle, empty compartment with silicon resin bond and the compartment filled with pebbles, is presented in Fig. 4. The insulation is protected by 0.5mm aluminum sheet on the outside. Dimensions of TES and the material properties of the components play important role for determining the energy storage capacity. The specification of the secondary TES is presented in Table 2.

3 Experimental Methodology

The experimental methodology comprises mainly of providing a measured Joule heating, measuring the mass flow rate of the air, and assessing the energy stored in secondary TES through temperature measurements. The schematic of the experimental layout is shown in Fig. 5. Joule heating is carried out by maintaining the current and voltage with variacs. A rotameter is used to measure the volumetric flow rate of the air. Temperatures at several locations are measured by using K-type

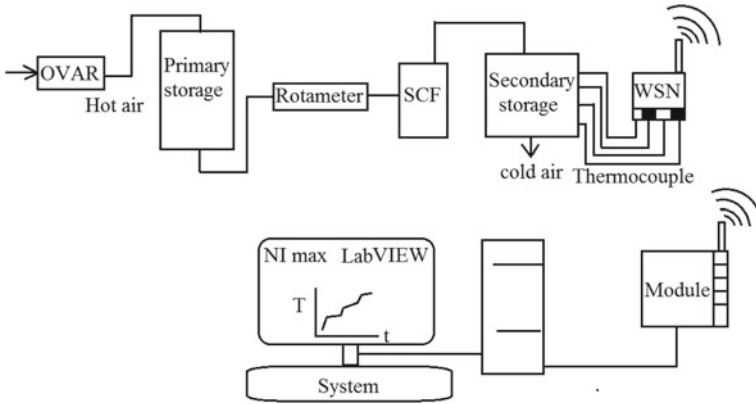


Fig. 5 Schematic of the experimental layout

thermocouples. National instrument wireless sensor board (WSN3212) is used to transmit thermocouple reading, and LABVIEW is used to monitor it online. The layout of the thermocouples will be described in detail next.

3.1 Temperature Measurement in TES

The temperature distribution within the secondary storage has been measured with respect to time while charging and discharging of the TES. This is carried out by using K-type thermocouples fixed at different locations. The schematic view of the secondary TES with layout of various thermocouples is shown in Fig. 6 with centerline indicated by dashed line. The four compartments of the secondary TES are denoted by C1, C2, C3, and C4. The thermocouples are placed inside the various component materials of the secondary TES to study the heat distribution.

The axial direction is indicated by z and radial direction by r . The axial and radial coordinates of the thermocouples in the r and z plane with respect to the centerline are summarized in Table 3. In order to measure the temperature of the pebbles which is the sensible thermal energy storage medium, two thermocouples are placed diametrically opposite inside each compartment. The average temperature reading of the two thermocouples is taken as pebble temperature for that compartment. Thus, in order to monitor the pebble temperature inside each compartment, eight thermocouples are used. To measure the metal baffles temperature, four thermocouples are placed at the surface of the metal, one in each compartment. Four thermocouples are placed in contact with the glass wool outer surface, one in each compartment. For measuring the aluminum casing temperature, only one thermocouple is used at the outer surface and mid-height of the TES ($z = 250$ mm). Thermocouples are also placed at the inlet and outlet of TES to record inlet and outlet air temperature.

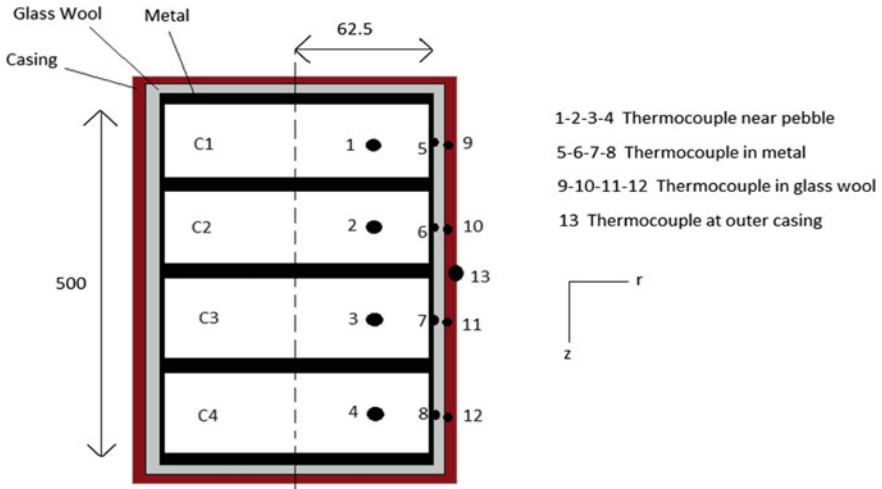


Fig. 6 Schematic view of secondary TES with thermocouple location

Table 3 Co-ordinates of thermocouple placement in the secondary TES

Compartment	Material	Pebble	Metal	Glass wool
	Axial location (z mm)	Radial location (r mm)		
C1	62.5	35	65.5	70.5
C2	187.5	35	65.5	70.5
C3	312.5	35	65.5	70.5
C4	437.5	35	65.5	70.5

3.2 Procedure

Blower is use to suck the ambient air, and the mass flow rate is set to a particular flow rate using the rotameter by adjusting the variable frequency drive blower. For performing the charging experiments, the air is heated by forced convection and supplied measured thermal energy in the form of Joule heating. Hot air enters the TES from the top during charging, and readings from all the thermocouples are recorded over the time. The flow path during the charging experiment is shown in Fig. 7.

After charging for a significant duration the thermal energy stored in TES is extracted by passing cold air flow through it. During discharging, with the help of the blower, ambient air is introduced from the bottom inside the charged (heated)

Fig. 7 Air flow path during charging

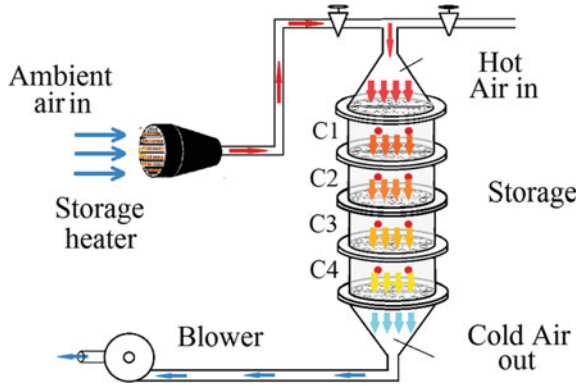


Fig. 8 Air flow path during discharging

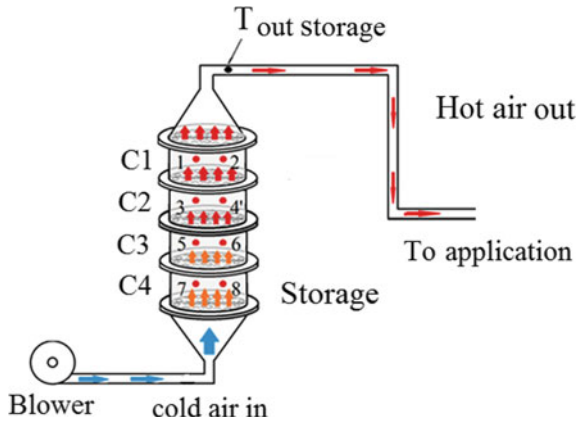


Table 4 Duration and mass flow rate during charging and discharging experiments

Parameter	Charging	Discharging
Time (sec)	12000	7000
Mass flow rate (kg/s)	0.0042	0.0042

TES. The data from the thermocouples are recorded till a significant amount of heat is taken away from the TES. The flow path during the discharging experiment is shown in Fig. 8. The mass flow rates during charging and discharging experimentation along with the time duration are provided in Table 4.

4 Experimental Results

4.1 Heat Loss in Pipe Flow

Even though the SATS is insulated with glass wool completely, there is heat loss. In order to measure the temperature drop, thermocouples are also set up at different locations. The temperature at outlet of heater is 260 °C, and at the inlet of storage is 150 °C. So there is around 110 °C drop of temperature while flowing from heater outlet to secondary TES inlet. This drop is observed over a length of 1.5 m of insulated pipe line which indicates a drop of 73 °C per meter. Thus, for improving the efficiency of the system, the heat loss needs to be reduced.

Next, the details of the charging and discharging of secondary storage are presented. Charging of the secondary TES is carried out for 11,900 s (three and half hours) followed by discharging for 7000 s (two hours). Thus, the total duration of experiments is approximately 7 h including initial preparation and running.

4.2 Pressure Drop in Secondary TES

The pressure drop in the secondary TES is also calculated using the pressure drop characteristics of rock beds with air as the heat transfer medium. At first, the porosity is calculated by filling a cylinder of known volume with pebbles and then filling up the cylinder with water. The volume of the cylinder and the volume of the water are used to calculate the porosity. Diameter of the cylinder is 0.125 m and length of the cylinder is also 0.125 m which results in volume of cylinder as 0.001533 m³. The amount of water required to fill the cylinder is thus 1.533 L. The amount of water required to fill the void of cylinder after filling the pebbles in cylinder is 0.6 L. The void fraction or porosity is calculated as 0.6/1.533 = 0.3913.

The pressure drop across the bed is given by Hänchen et al. (2011)

$$\Delta p = \frac{LG^2}{\rho_f d} \left(150 \frac{(1 - \epsilon)}{\epsilon^3} \frac{\mu_f}{Gd} + 1.75 \frac{(1 - \epsilon)}{\epsilon^3} \right) \tag{4}$$

where

Δp = pressure drop (Pa)

L = height of the storage (m)

ρ_f = density of fluid (kg/m³)

G = mass flow per unit cross section (kg/(m²s))

ϵ = porosity

δq = latent heat of fusion (J/kg)

μ_f = dynamic viscosity of fluid (Pa-s)

Fig. 9 Secondary storage charging: temperature rise of pebbles in the compartment with time

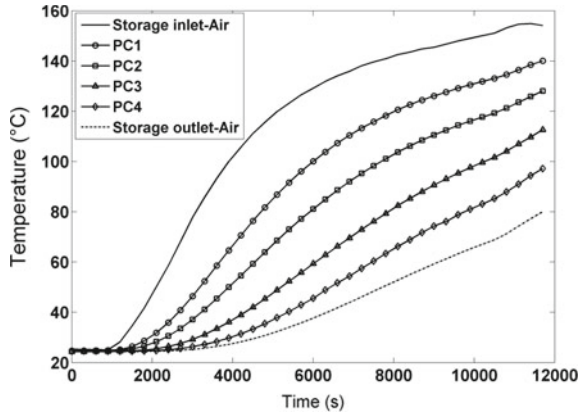
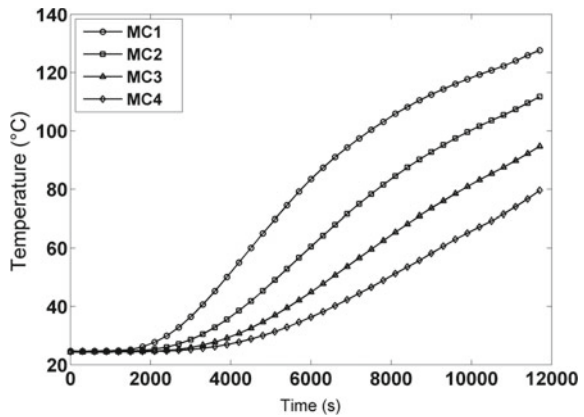


Fig. 10 Secondary storage charging: metal compartment wall temperature



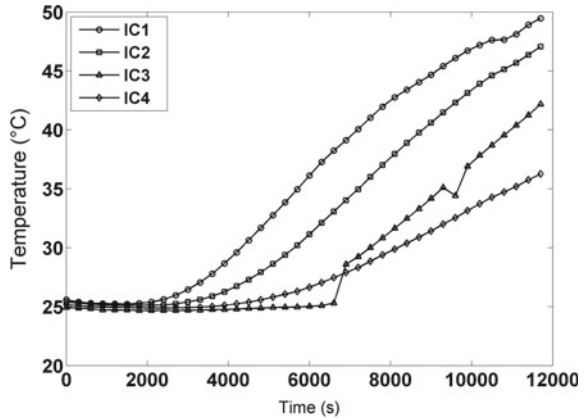
For the mass flow rate of 0.0042 kg/s and considering the parameters of secondary storage, the pressure drop in secondary storage is approximately 62 Pa.

4.3 Charging of Secondary TES

Ambient air is sucked in through the blower and heated by Joule heating. A constant mass flow rate of 0.0042 kg/s is used to charge the secondary TES. Hot air enters from top of the storage, and heat is transferred from air to the pebble by forced convection. The temperature distribution which is indicator of the energy stored is measured with help of thermocouples placed inside as described earlier.

The temperature recorded by the thermocouples at different locations is presented in Fig. 9. It is observed that the temperature at the inlet of the secondary storage is at the ambient temperature initially up to 1000s and then increases rapidly. This is

Fig. 11 Secondary storage charging: insulation temperature



due to the fact that initially, the SATS piping is at ambient temperature so the heat is transferred from the hot air to the pipe causing temperature at inlet of the storage to be almost same as ambient air. As the time passes, the difference in temperature between fluid and pipe decreases so temperature at the inlet of storage increase. With time the pebble temperature in all the four compartments indicated by PC1, PC2, PC3, and PC4 are seen to be increasing in Fig. 9. In compartment C1, temperature increases from 25 °C to 140 °C, in C2, temperature increases from 25 °C to 130 °C, in C3, temperature increases from 25 °C to 110 °C, and in C4, temperature increase from 25 °C to 100 °C. Temperature in compartment 1 and 2 increases rapidly up to 6000s because the hot fluid has more enthalpy with it compared to the pebbles. As the hot air flows down, it’s enthalpy decreases so rise in temperature in compartment 3 and 4 is lesser.

The temperature rise over time in the metal compartments of TES is shown in Fig. 10. It follows the same trend as the pebbles in different compartments. It can be again observed that there is no appreciable temperature rise in the first 2000 s. Figure 11 shows the temperature inside the insulation of secondary TES for different compartments. Temperature rise in the thermal insulation is observed to be quite less as compared to the metal walls of the TES.

One thermocouple is placed at the outer surface of casing (at mid-height of the storage system), and one thermocouple is left exposed in ambient air to measure the casing and ambient temperature, respectively. The two temperatures are shown in Fig. 12. The casing temperature is observed to increase from 25 °C to 33 °C and ambient temperature increases from 25 °C to 27 °C during the entire duration of the charging experiment. The outer casing temperature is not significantly higher than ambient temperature at all times during the experiment. Thus, convective and radiative heat losses can be neglected. However, from all the temperature graphs, it can be observed that steady state of the secondary TES is not attained even after 3.5 h. The experiments could not be carried further due to malfunction of Joule heating.

Fig. 12 Secondary storage charging: casing and ambient temperature

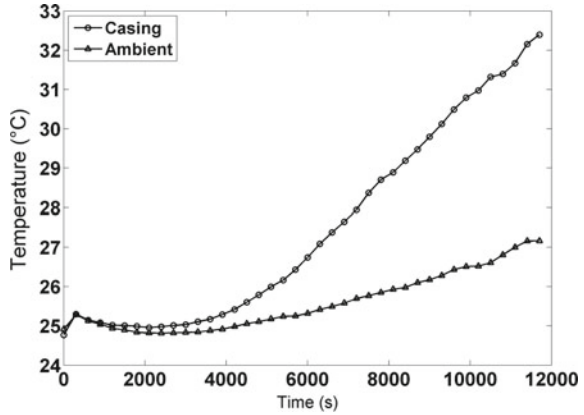
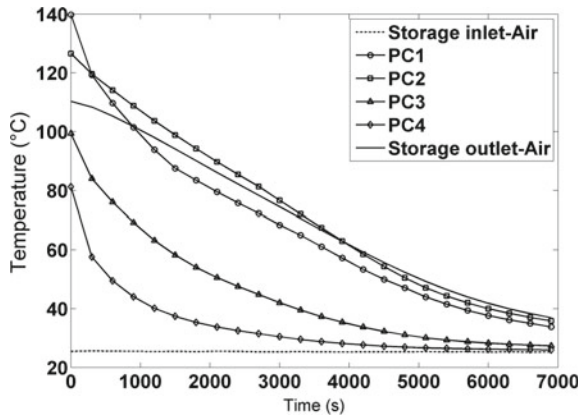


Fig. 13 Secondary storage discharging: temperature drop of pebbles in the compartment with time



4.3.1 Discharging of Secondary TES

After charging for a period of about 11900s, discharging of TES is started by reversing air flow. Ambient air is sucked by blower and is made to enter into the secondary TES from bottom. Discharging is carried out for a period of about 7000s, and mass flow rate is kept same as in charging, i.e., 0.0042 kg/s.

Figure 13 shows the thermocouple readings at the inlet of the TES (bottom of TES), exit of TES (top of TES), and the pebbles in different compartments. The temperature of pebbles in compartment 3 and 4 decreases more rapidly in comparison to the pebble temperature in compartment 1 and 2 because the ambient air first comes in contact with pebble of C4 and C3. As the air heats up, the temperature difference between air and pebble of C1 and C2 decreases so heat transfer rate decreases. It is also observed that the temperature of the hot air from the secondary TES outlet decreases with time from approximately 110 °C to 50 °C. Steady state is achieved for pebbles in compartment 3 and 4 at around 6500 s. The temperature of pebbles in

Fig. 14 Secondary storage discharging: temperature drop of metal walls in the compartment with time

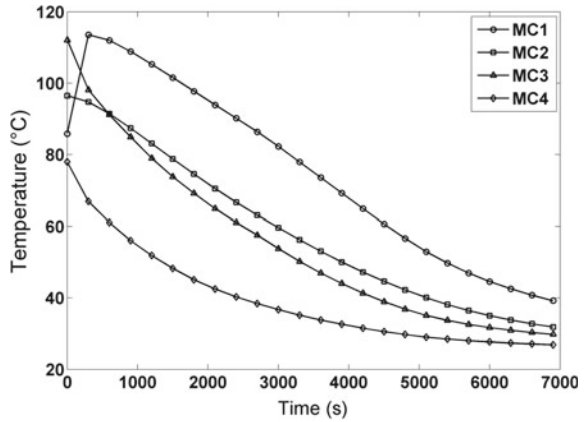
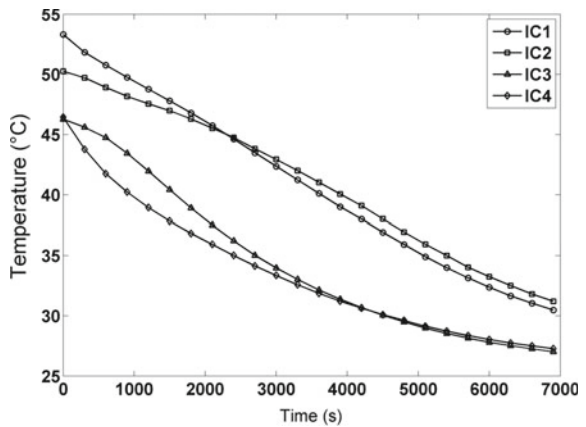


Fig. 15 Secondary storage discharging: temperature drop in insulation in the compartment with time



C1 and C2 still continues to drop indicating that these compartments are not fully discharged. Due to decreasing temperature difference between the ambient air and pebbles in compartments (C1 and C2), complete discharge will take excessive time, and the experiments are stopped around 7000 s.

The temperature of the metal walls of the compartments during discharging is shown in Fig. 14. It also follows the same trend as the pebble but in the compartment, 1 rise in temperature is observed up to 1000 s. Figure 15 shows the temperature drop with time in the insulation of the compartments. It is observed that insulation temperature in compartments 3 and 4 are almost similar. The insulation temperature in compartment 1 and 2 are also similar and approximately 10 °C higher than the temperature in the compartments 3 and 4.

5 Energy Balance

In this section, an approximate of the energy stored in the secondary TES is estimated using the measured temperatures and the material properties available from the literature. The properties are taken at a constant temperature in order to simplify the calculations and are presented in Table 5.

The geometrical dimensions of the various components of the secondary TES are known. Using the dimensions and density, the approximate mass of each TES constituent such as pebbles, metal structure, thermal insulation (glass wool), and outer metal casing is computed. Using the approximate mass and temperature rise of the material, an approximate energy balance is arrived at assuming steady state, i.e., at the end of the charging 7000 s). It is to be noted here that neither steady state is attained nor the mass of the materials very precise. However, this helps to have a qualitative idea of the heat storage distribution. Table 6 gives a qualitative overview of the energy balance of the secondary TES. It is observed that approximately 60% of the inlet energy leaves out of the TES with the outgoing fluid. Only 12% of the incoming thermal energy is stored in the pebbles. The metal components such as the metal compartment, baffles, and nut bolts store almost around 17% of the incoming energy. The energy stored by metal components is higher as the secondary TES is small in size and is mainly used for recovering waste heat. As expected, the energy stored in insulating material is negligible.

Table 5 Properties at average temperature 80°C

Parameter	Notation	Value
Density of pebble(kg/m ³)	ρ_s	2200
Specific heat of pebble(J/kgK)	c_s	710
Pebble diameter(m)	d	0.02
Thermal conductivity of pebble(W/mK)	k_s	1.83
Porosity	ε	0.39
Density of metal casing(kg/m ³)	ρ_m	7200
Specific heat of metal casing(J/kgK)	c_{pm}	500
Thermal conductivity of metal casing (W/mK)	k_m	50
Density of air(kg/m ³)	ρ_f	1
Specific heat of air (J/kgK)	c_{pf}	1009
Thermal conductivity of air (W/mK)	k_f	0.0299
Thermal conductivity of insulation (W/mK)	k_{in}	0.04
Mass flow rate (kg/s)	\dot{m}	0.0042
Velocity (m/s)	v	0.276
Prandtl no.	Pr	0.7

Table 6 Energy balance of the secondary TES

Enthalpy of fluid at inlet of storage	630 W
Enthalpy of fluid at outlet of storage	378 W
Charging power (enthalpy lost by fluid)	252 W
Energy stored by pebble in C1	23.12 W
Energy stored by pebble in C2	21.11 W
Energy stored by pebble in C3	17.09 W
Energy stored by pebble in C4	15.08 W
Energy stored by metal in C1	22 W
Energy stored by metal in C2	17.85 W
Energy stored by metal in C3	15.75 W
Energy stored by metal in C4	11.55 W
Energy stored by nut bolt	25 W
Energy stored by baffle	17 W
Energy stored by glass wool	1 W
Heat loss in convection and radiation	3 W
Difference in energy balance	62 W

6 Conclusion

The experimental results of a secondary TES are presented in this work. Temperature readings of the TES components are presented while charging and discharging of the TES using air as working fluid. It is found that the SHTES using pebbles enclosed within metal container performs well. The system can be used to store waste heat after metal processing, and the stored heat can be extracted while discharging. The heat losses from the setup have to be minimized. Further, improvements have to be carried out in the setup to enable to attain steady state while charging. This work is a first demonstration of the use of locally available material to construct a SHTES system and can be considered as proof of the concept.

References

- Ávila Marín AL (2011) Volumetric receivers in solar thermal power plants with central receiver system technology: a review. *Solar Energy* 85(5):891–910
- Blanco M, Miller S (2017) Introduction to concentrating solar thermal (CST) technologies. In: Blanco MJ, Santigosa LR (eds) *Advances in concentrating solar thermal research and technology*. Woodhead Publishing Series in, Energy. Woodhead Publishing, pp 3–25
- Fath HE (1998) Technical assessment of solar thermal energy storage technologies. *Renew Energy* 14(1):35–40 (6th Arab International Solar Energy Conference: Bringing Solar Energy into the Daylight)

- Häberle A (2012) Concentrating solar technologies for industrial process heat and cooling. In: Lovegrove K, Stein W (eds) Concentrating solar power technology. Woodhead Publishing Series in, Energy. Woodhead Publishing, pp 602–619
- Hänchen M, Brückner S, Steinfeld A (2011) High-temperature thermal storage using a packed bed of rocks-heat transfer analysis and experimental validation. *Appl Thermal Eng* 31(10):1798–1806
- Hoffschmidt B, Te'llez FM, Valverde A, Ferna'ndez J, Ferna'ndez V (2003) Performance evaluation of the 200-kWth HiTRec-II open volumetric air receiver. *J Solar Energy Eng* 125(1)01:87–94 NREL. DNI Map of India
- Patidar D, Pardeshi R, Chandra L, Shekhar R (2017) Solar convective furnace for heat treatment of aluminium. *Lecture Notes in Mechanical Engineering*, pp 1531–1541
- Patidar D, Tiwari S, Sharma P, Chandra L, Shekhar R (2015) Open volumetric air receiver based solar convective aluminum heat treatment furnace system. In: *Energy procedia*, vol 69, pp 506–517. International Conference on Concentrating Solar Power and Chemical Energy Systems, SolarPACES 2014
- Pielichowska K, Pielichowski K (2014) Phase change materials for thermal energy storage. *Progress Mater Sci* 65:67–123
- Pitz-Paal R, Hoffschmidt B, Böhmer M, Becker M (1997) Experimental and numerical evaluation of the performance and flow stability of different types of open volumetric absorbers under non-homogeneous irradiation. *Solar Energy* 60(3):135–150
- Powell KM, Edgar TF (2012) Modeling and control of a solar thermal power plant with thermal energy storage. *Chem Eng Sci* 71:138–145
- Sarbu I, Sebarchievici C (2018) A comprehensive review of thermal energy storage. *Sustainability* 10(1):191
- Sharma P, Sarma R, Chandra L, Shekhar R, Ghoshdastidar P (2015) Solar tower based aluminum heat treatment system: part i. Design and evaluation of an open volumetric air receiver. *Solar Energy* 111:135–150
- Sharma P, Sarma R, Chandra L, Shekhar R, Ghoshdastidar P (2014) On the design and evaluation of open volumetric air receiver for process heat applications. In: *Energy Procedia*, vol 57, pp 2994–3003. 2013 ISES Solar World Congress
- Tian Y, Zhao C-Y (2013) A review of solar collectors and thermal energy storage in solar thermal applications. *Appl Energy* 104:538–553